JTTEE5 19:1001–1012
DOI: 10.1007/s11666-010-9482-3
1059-9630/$19.00 © ASM International

Microstructural Study of Splat Formation for HVOF Sprayed NiCr on Pre-Treated Aluminum Substrates

S. Brossard, P.R. Munroe, and M.M. Hyland

(Submitted November 19, 2009; in revised form January 21, 2010)

In this study, the mechanisms of splat formation and the influence of substrate surface conditions were studied for NiCr splats HVOF sprayed onto Al. The specimens, having undergone various substrate pre-treatments, were observed at high resolution using various electron microscopy techniques with emphasis on the splat microstructure and the splat-substrate interface. From the observations made here, a model for splat formation is proposed, whilst the effects of surface chemistry on this process were investigated. It was found that that due to the deformation of the substrate on impact of the partially molten particle, effective contact may be achieved between the substrate and the splat. However, in many cases, much of the initial projected particle did not adhere to the substrate after impact. The presence of oxide or hydroxide layers on the surface of the substrate was influential on the adhesion of the NiCr splat

Keywords aluminum, HVOF spray, interface, nickel chromium, oxide, splat

1. Introduction

Understanding of splat formation in the High Velocity Oxy-Fuel (HVOF) spraying process is a key step in the design of coatings with improved properties and performance.

The HVOF spray process is a relatively recent development compared to many other spray processes, and the characteristics of the coatings produced by this method, such as high bond strength and thickness capacity, relatively low porosity and oxide contents, etc., make it a competitive alternative for the production of coatings in many industries (aerospace, industrial gas turbine, petrochemical/gas industries, automotive industry, etc.).

The HVOF system operates through the injection of a powder in a stream of combusted gases, a mixture of oxygen and a fuel gas (hydrogen, heptane, kerosene, etc.). Depending on the powder feedstock (material type and powder size) and the spray conditions (temperature of the flame and velocity of the carrier gas), the sprayed particles may impact the substrate with a range of velocities (usually 400-800 m s^{-1}) and variable state (from completely solid to fully melted) (Ref 1, 2). This may create a variety of splat types (solid, partially melted, or fully melted). The splat morphology will also depend on the properties of substrate, such as its hardness and roughness (Ref 3). Depending on the spray conditions, it is possible to create coatings with a bimodal structure, consisting of a mixture of melted and non-melted zones (Ref 4-6).

Although the microstructure of fully prepared coatings has been widely studied (Ref 4-6), little study has been performed regarding the microstructure and formation of single splats prepared by the HVOF spray process.

However, some parallels may be drawn between the HVOF process and other spray processes. The formation of fully melted splats may be compared to the splat formation in the plasma spray process, which has been more widely studied and modeled (Ref 7). Similarly, the situation where the particles impact the substrate in a non-melted state can be linked to the cold spray process, where there have also been a significant number of studies performed (Ref 8-10). However, often in HVOF, sprayed particles may impact the substrate in a partially melted state. For example, Trompetter et al. observed the occurrence of the different types of splats and the influence of substrate hardness by spraying NiCr onto a range of substrates. It was found that increasing the substrate hardness increased the proportion of melted splats, as the kinetic energy is dissipated upon impact less in the deformation of the substrate and more in heating and deformation of the sprayed particle. However, the microstructure of such splats at its interface with the substrate was not described in detail (Ref 3). The coating-substrate interface, however, was examined for a WC-Co coating HVOF sprayed onto a Cu substrate by Guilemany et al. They observed a thin layer of fine-grained materials at the interface with the substrate, which they interpreted as evidence of substrate melting (Ref 11). However, this study concerned a relatively thick coating and not single splats. Finally, Sobolev and Guilemany studied the effect

S. Brossard and **P.R. Munroe**, School of Materials, University of New South Wales, Sydney, NSW 2052, Australia; and **M.M. Hyland**, Chemical & Materials Engineering Department, University of Auckland, Auckland 1142, New Zealand. Contact e-mail: sophie.brossard@student.unsw.edu.au.

of oxidation of the particle on the splat formation: they showed that effects may include thicker and smaller splats having less effective contact with the substrate due to a decrease in the build-up in pressure upon impact, although dissolution of oxygen within the splat was thought to increase its wetting on the substrate (Ref 12).

This study also aims to investigate the influence of pre-treatments (such as heat-treating and boiling), inducing differences in the surface conditions (via variations in surface chemistry and roughness), on the splat morphology and the interaction with the substrate. Indeed, for the case of plasma spray, surface chemistry and roughness have been shown to have a significant influence on the splat formation. For example, in the case of oxidized steel substrates, Cedelle et al. found that plasma-sprayed nickel particle had a better wetting and smaller spreading time, giving flatter splats, compared to non-oxidized steel substrates (Ref 13). For Al, previous studies in the case of plasma-sprayed NiCr showed that preheating the aluminum substrate resulted in slightly flatter and less fragmented splats; it was also observed that on boiled substrates, on which a thick (of a few hundred nm) hydroxide layer is formed, no splats would adhere (Ref 14, 15). Explanations for these various effects included the occurrence of gas release from the substrate, notably water from the (partial) dehydration of the Al hydroxide, which could hinder the splat adhesion, and this study intends to enquire on such effects for the case of HVOF spraying.

In this study, a NiCr powder was sprayed by HVOF onto aluminum substrates that, prior to spraying, were subjected to different pre-treatments: polishing, heat-treating and/or boiling. A range of microscopy techniques were used to observe the splat morphology, microstructure, and the nature of the interface with the substrate for four Al specimens with different surface pre-treatments, to investigate how the surface chemistry may affect the splat formation in the case of the HVOF spraying process.

2. Experimental Procedure

Four different substrates were used; all prepared from a 5052 aluminum alloy. These are listed in Table 1.

All substrates were firstly mechanically ground and mirror polished with diamond paste, to a nanoscale roughness (measurement of the roughness were made for similar substrates for another study by the same authors and details can be found in the relevant publication, Ref 14) were made. The boiled substrates were placed into boiling distilled water for 30 min, while the thermally treated substrates were heated at 350 °C for 90 min in air. The aim of these treatments is to form surface oxides (or hydroxides for the boiled specimens) and/or to induce some level of surface roughness.

Table 1 Substrate nomenclature and condition

Specimen	Substrate	Pre-treatment
Al_P	Aluminum 5052	Polished (to nanoscale smoothness)
Al_PT	Aluminum 5052	Polished and thermally treated
Al_B	Aluminum 5052	Boiled
Al_BT	Aluminum 5052	Boiled and thermally treated

The sprayed material was a commercial NiCr alloy powder (Ni80-Cr20, (−45 +5) μm) (Sulzer Metco 43 VF-NS, Wohlen, Switzerland). HVOF spraying was carried out with a Sulzer Metco (Wohlen, Switzerland) Diamond jet (DJ-2600) gun, fueled with air at 160 psi, oxygen and propylene at 110 psi, the flow rates being 744, 419, and 128 SCFH, respectively. The feeding rate of the powder was of 26 g/min, the carrier gas being nitrogen at 140 psi. Five swipe passes were made, at the velocity of 0.4 m s^{-1}, and at a spraying distance of 266 mm. HVOF spraying was performed at room temperature.

The specimens were then characterized using a range of analytical techniques. A scanning electron microscope (SEM) (Hitachi, S3400-X, Mito, Japan) was used to image the overall morphology of the splats and the substrates. A focused ion beam microscope (FIB) (FEI, xP200, Hillsboro) was used to mill cross sections of the splats using an energetic gallium ion beam, and to image them using secondary electrons induced by the ion beam. Details have been described elsewhere (Ref 16). A dual beam microscope (that is a FIB and SEM combined into a single instrument) (FEI, xT Nova Nanolab 200, Hilssboro) was used to prepare cross sections of splats (100-200 nm in thickness) suitable for transmission electron microscope (TEM) observation. These were prepared using the lift-out method as described elsewhere (Ref 16) and examined in a TEM (Philips, CM200, Eindhoven, The Netherlands) to which energy dispersive x-ray spectroscopy (EDS) facilities have been interfaced.

Several FIB and TEM cross sections were made and studied, at least one for each particular feature and/or type of splat, but for the sake of brevity only representative images will be presented here. The process of cross section preparation also involves the in situ deposition of a layer of platinum on top of the splat prior to milling to protect the outer surface of the splat from ion beam damage. This layer is then present, and labeled, on the images obtained.

3. Results and Discussion

3.1 Description of the Splats Observed on the Polished and Polished and Thermally Treated Specimens

Figure 1 displays SEM images of the different types of splats found on the polished (Al_P) and polished and thermally treated (Al_PT) substrates. When the NiCr particles impact on the Al substrate, they create a crater in the substrate that can be observed on all the splat-substrate cross sections examined. Figure 1(a) shows such a crater where the NiCr has not adhered to the substrate. The uneven surface of the crater, relative to the surrounding substrate, is clearly visible.

The splats observed on Al_P and Al_PT substrates were, generally, similar and exhibited the following characteristics:

- Some splats were formed from NiCr that was only partially melted. Figure 1(b) shows an example of such splat: it appears to be composed of unmelted fragments (marked 1 on Fig. 1b) within a melted matrix. These splats will be denoted as ''partially molten splats.''
- Other splats were formed from NiCr particles that were fully melted, as shown by the less granular structure compared with the previous type of splat (Fig. 1b). Two types of these splats can be distinguished: on one hand, splats which appear to have broken into several fragments, such as the splat shown in Fig. 1(c) and on the other hand, splats which appear to have fractured less and adhered to the impact crater, see Fig. 1(d), such that it forms almost a fully disc-shaped splat. A central pore may be present in some splats, such as the one shown in Fig. 1(e). All of these splats will be denoted here as ''fully molten splats.''

3.1.1 Structure and Formation of the Fully Melted Splats. *Observation of FIB and TEM Cross Sections of the Splats:* Figure 2, a FIB cross section made across a fully melted fragmented splat, similar to the one shown in Fig. 1(c), is presented. The cross section of the crater from the impact of the NiCr can be clearly seen and is about 4 μm in depth (marked 1). The splat-substrate interface is irregular in shape (1), and one can note that the Al substrate has been lifted up above the initial substrate surface at the periphery of the crater (2). This suggests that the aluminum substrate had undergone some localized melting in addition to being deformed.

Moreover, zones bereft of NiCr (3) were found between NiCr fragments, which display a quite irregular and coarse grain structure (4). On top of the NiCr region, a thin layer (~50-100 nm) was observed (5). This layer was identified by TEM as being a chromium oxide (see description of the TEM cross section presented in Fig. 4).

Figure 3 shows a FIB cross section of a non-fragmented fully melted splat, similar to the splat shown in Fig. 1(d). The splat-substrate interface is still irregularly shaped (1), but to a lesser degree compared to the fragmented splat shown in Fig. 2. The contact between splat and substrate is also good, except in the center of the splat (2) where some delamination seems to have occurred. Furthermore, the grain structure of the splat is very fine ($d < 0.5$ μm) and columnar (3).

Finally, Fig. 4 presents a TEM cross section of a fully melted splat. Again the splat-substrate interface is very irregular (1), with the Al substrate being lifted up at the periphery of the crater (2), but, in some areas, the splat-substrate interface is also quite indistinct (1): an EDS linescan performed across the interface (marked L1, Fig. 4f) shows that Ni has diffused into the substrate to a depth of about 150 nm (3). This confirms the occurrence of substrate melting. On closer inspection of the interface,

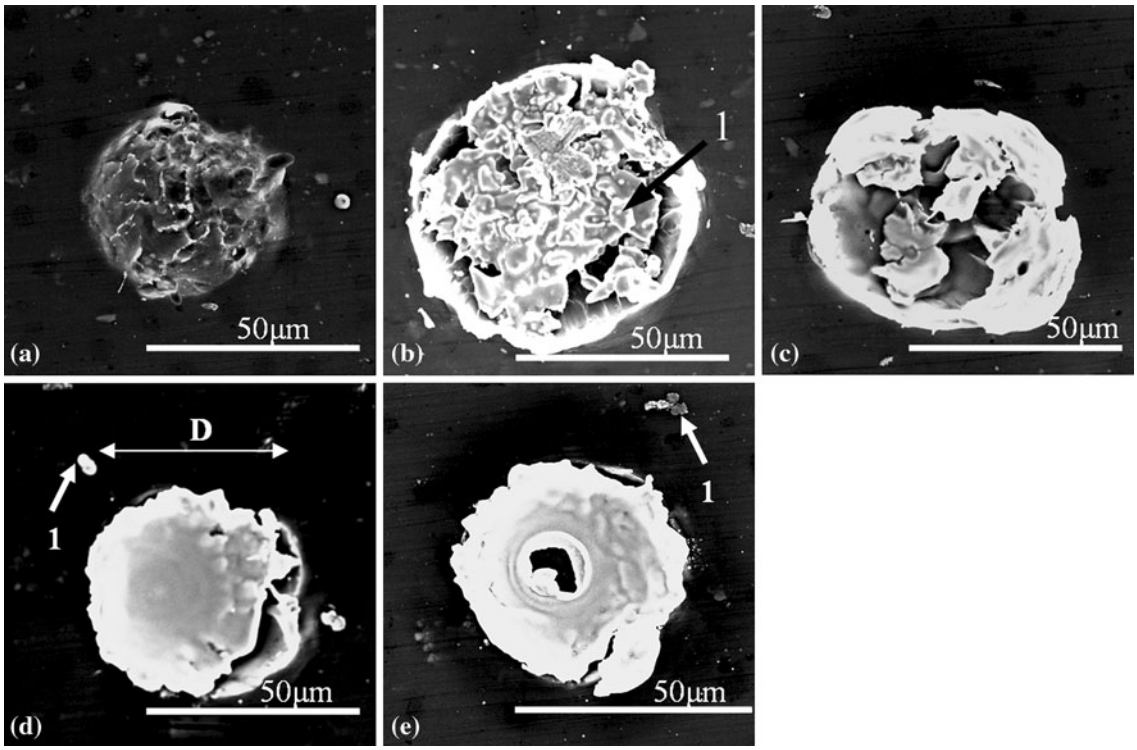

Fig. 1 SEM images of (a) a substrate crater, and different types of splats found on Al_P and Al_PT: (b) partially melted splat, (c) fragmented fully melted splat, (d) non-fragmented fully melted splat, (e) non fragmented fully melted splat with a central pore

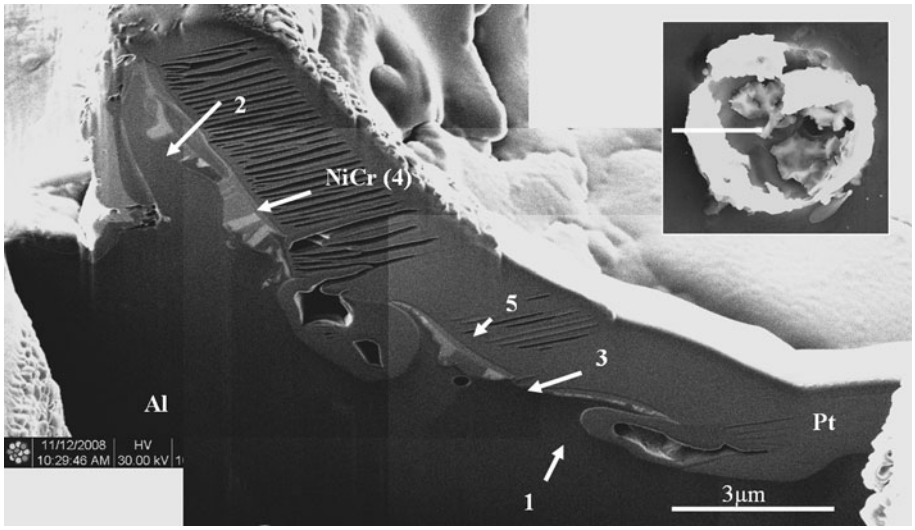

Fig. 2 FIB cross section of a fragmented and fully melted splat (the inset image shows an image of the splat in plan view before sectioning) from Al_PT

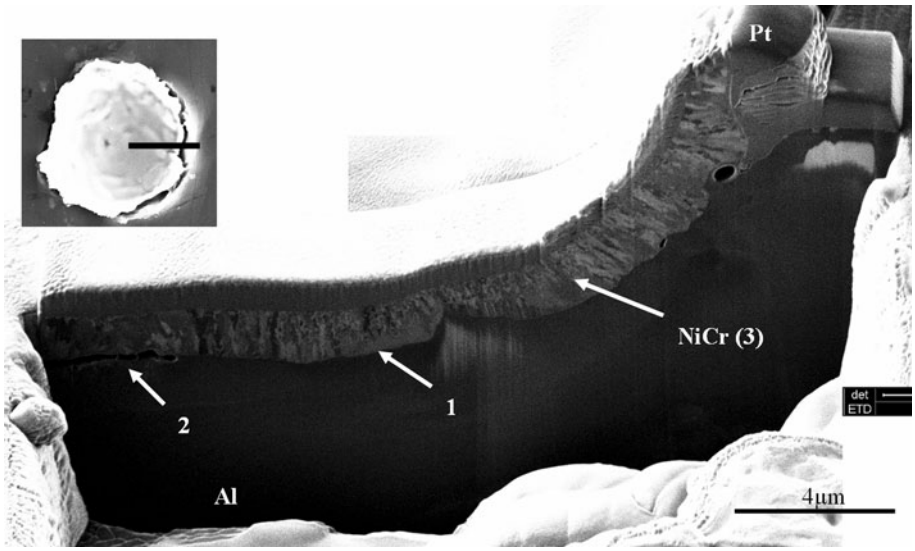

Fig. 3 FIB cross section of a fully melted splat (see inset image) on Al_PT

a fine grained structure was observed within the substrate (4): NiCr appears to have intermixed with the molten Al substrate, which was jetted within the splat, but as the solid solubility of Ni in Al is extremely limited (Ref 17), it may have frozen in the fine grained microstructure observed. The fact that the variation of Al and Ni concentrations, as measured by the linescan across the splat-substrate interface, is gradual suggests that this is not a stoichiometric intermetallic phase. This is contrary to observations, for example, by Kitahara and Hasui for plasma spray of Ni onto Al substrates (Ref 18). Moreover, diffraction patterns taken from this phase exhibited reflections which prevented unambiguous identification. Consequently, the structure observed may more likely be a very fine grained metastable mixture of a non-equilibrium Ni-Al phase formed due to the rapid solidification of the aluminum substrate into which some Ni has dissolved. Finally, on the outer surface of the splat, the layer observed (5) was identified by both EDS mapping (see Fig. 4d, e) and electron diffraction as Cr_2O_3 (see diffraction pattern Fig. 4g).

From other TEM cross sections made on similar splats, it was found that other oxide phases can also be present, such as NiO and $NiCr_2O_4$. These are both usually located not only on the outer surface of the splat, but also at the periphery of the splat or in pores at the interface. Al_2O_3 was also observed, mostly in pores at the splat-substrate interface.

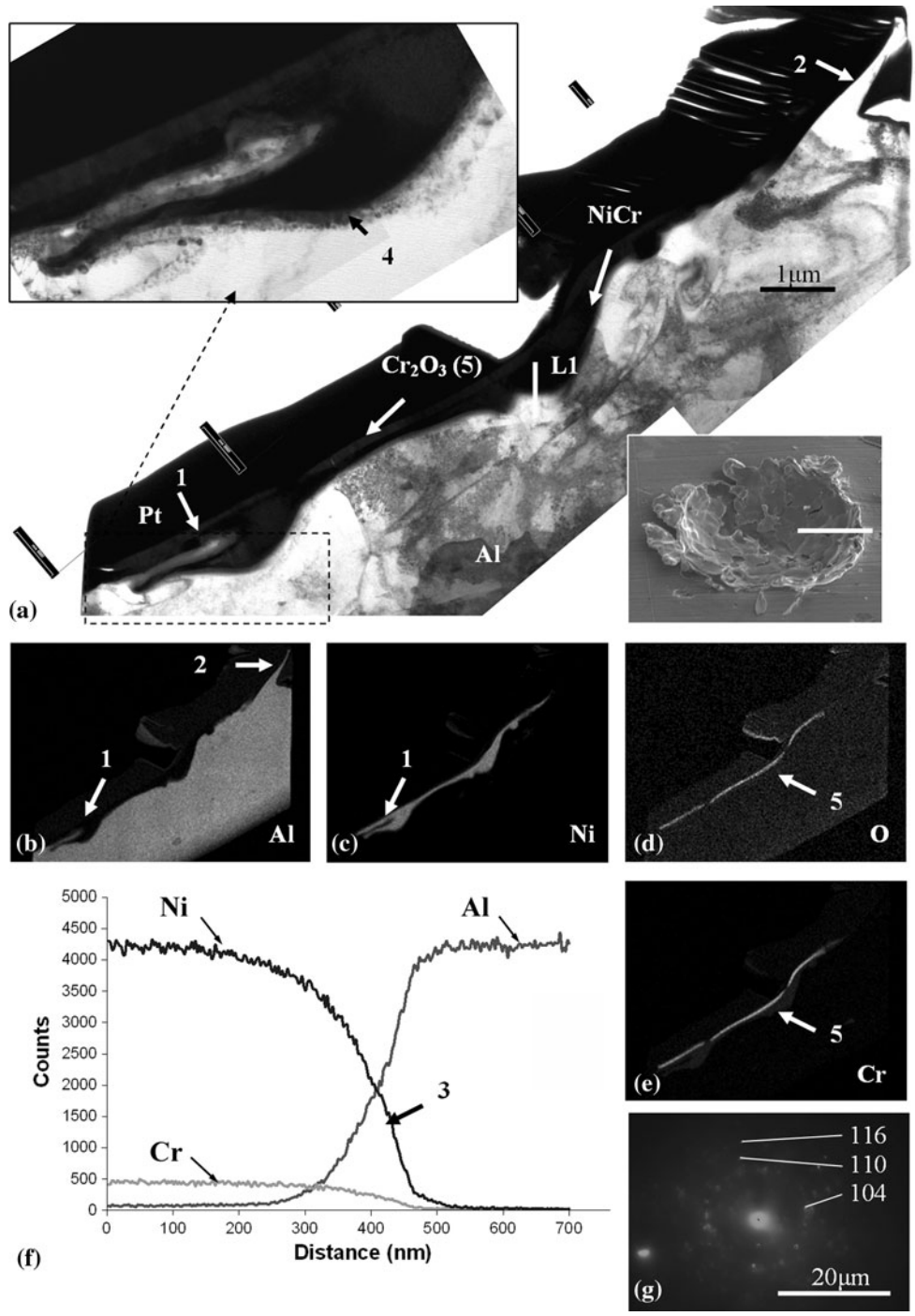

Fig. 4 TEM cross section of a fully melted splat (see inset image) from the Al_PT specimen: (a) bright field image, (b) elemental EDS maps for Al, (c) Ni, (d) O, (e) Cr, (f) linescan across the splat-substrate interface, (g) diffraction pattern of Cr_2O_3

One can note that for all these cross sections, it appears that the splat only partially fills the crater, which itself is smaller in diameter than the initial sprayed particle. For example, for the splat presented in Fig. 3: by measuring the radius R_c of the crater and the depth h_c, and approximating this as a fraction of a sphere, the volume V_c of the corresponding sphere can be calculated by the expression $V_c = \frac{4}{3}\pi\left(\frac{R_c^2+h_c^2}{2h_c}\right)^3$. The initial sprayed particle is expected to be at least equal to V_c, thus here at least 164×10^3 μm^3. However, the volume of the deposited splat V_s, calculated by measuring its radius R_s and thickness h_s, can be

calculated by $V_s = \pi R_s^2 h_s$, and is evaluated here to be around 2.5×10^3 μm^3, thus only ~1.5% of the initial particle volume. This consequently shows very low deposition efficiency, at least with respect to the deposition of the first layer of splats (values are usually expected to range from 30 up to 90%, Ref 19, 20). Nevertheless, it is possible that for additional layers of splats, which will then deposit on NiCr and not on stainless steel, the deposition efficiency may be higher.

Description of the Formation Process: In the plasma spray process, particles impact on the substrate in a fully melted state, and no deformation of the substrate is observed. Here, for the HVOF process, FIB and TEM cross sections have shown that the splats characterized by the presence of a deep semi-spherical crater, due to the deformation of the substrate upon impact of the sprayed NiCr particle. This suggests that the particles were, therefore, not fully molten upon impact.

Zhang et al., upon HVOF spraying Inconel powder, explained the bimodal structure of the coating, comprising a mixture of melted and non-melted zones, by considering that the spay particle was partially melted and comprised a solid core surrounded by molten material (Ref 21).

Figure 5 presents a schematic representation of the formation of a fully melted splat: upon impact, the substrate is deformed by the solid core of the partially melted NiCr particle (Fig. 5a).

From the FIB and TEM cross sections, it appears that only a limited amount of the NiCr particle has adhered to the substrate. This leads to the conclusion that the non-melted core of the particle has most probably rebounded from the substrate after impact, while some of the melted particle has adhered to the substrate. This is shown in Fig. 5(b). Melted segments of the particle may also be splashed away from the splat during formation. Such fragments may either fall away from the substrate (which is sprayed while being held in a vertical position), or fall back on the substrate and form very small splats (see, e.g., the particles marked 1 on Fig. 1d, e). Such splashing phenomena is consistent with what is often observed for plasma spray (Ref 22, 23).

FIB and TEM cross sections also showed signs of localized substrate melting: that is, irregular splat-substrates interface (see Fig. 2(1), 4(1)), jetting of Al at the periphery of the crater (see Fig. 2(2), 4(2)), and mixing of Ni and Al at the interface (see Fig. 4L1), forming a very finely grained non-equilibrium structure. Such melting may be expected as the melting point of NiCr (~1400 °C) is significantly higher than that of Al (~649 °C).The manner in which the particle impacts on the substrate, that is involving a high kinetic energy, and deformation of the substrate, ensures very good contact between the particle and the substrate. Structural features that may usually limit such contact, such as the presence of an oxide layer or the desorption of adsorbates/condensates from the substrate surface which cause the release of gases upon impact (Ref 7, 14, 24), are here of lesser importance because of the high pressure applied by the impacting particle on the substrate.

Subsequently, the Al substrate is locally melted at the splat-substrate interface in the crater, due to the flowing movement of the melted splat. The Al substrate may also get jetted within the splat and/or on the sides of the crater (see (1) on Fig. 5b). Such jetting was observed in other cases where the impacting particle is, for the most part, solid upon impact, such as in cold spray (Ref 9) or, in certain conditions, HVAF (Ref 25). However, jetting occurs here more frequently and at a significantly greater scale.

Finally, various oxides may form due to the presence of hot gases, possibly from the HVOF flame, such as Cr_2O_3 which is found as a thin layer on the outer surface of the splat, or NiO and $NiCr_2O_4$ when they are found on the outer surface of the splat as well. Oxides found in pores at the splat-substrate interface such as NiO and Al_2O_3, may form, however, due to the presence of gas released from the substrate upon heating by the spraying process. Such phenomenon of desorption of adsorbates/condensates has been studied in more detail in plasma spray studies (Ref 14, 26-28).

3.1.2 Structure and Formation of the Non-Melted/ Partially Melted Splats. *FIB and TEM Observations:* Figure 6 shows a cross section prepared by FIB across a partially melted splat, similar to the splat shown in Fig. 1(b). A mix of non-melted particles, which exhibit a coarse grain structure (with a diameter, D, ~1 to several μm in diameter) (1) and fully melted zone, with a finer grain structure ($d < 0.5$ μm) (2), can be observed. Large pores are present (3), formed from the cavity between the non-melted particles, that is a region not fully filled by the melted NiCr. However, where some NiCr has melted, the contact between splat and substrate is good (4). Furthermore, the crater made by the deformation of the substrate upon impact can be seen to be around 3 μm in depth (4). Also, as seen for the fully melted splats, comparing the volume of the NiCr splat with the size of the crater, which indicates the initial size of the NiCr particle, suggests that the splat only represents a fraction of the initial NiCr particle. Indeed, from the FIB image, the NiCr particle creating such crater of depth of about 7 μm and diameter of about 22 μm should have a volume of at least 231×10^3 μm^3, while the volume of the splat itself is estimated to be around 2×10^3 μm^3, which thus represents only about 0.8% of the initial particle. This means

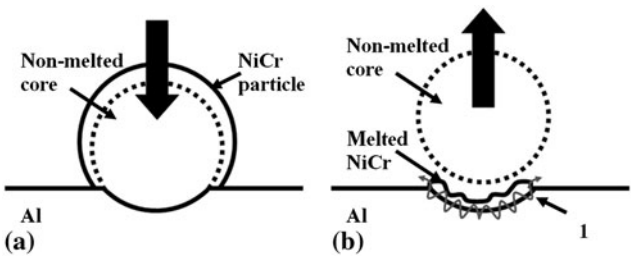

Fig. 5 Schematic representation of (a) a Ni-Cr particle impacting on the aluminum substrate and (b) the formation of a fully melted splat

that a large fraction of this particle must have rebounded away from the substrate.

TEM studies of these splats, although somewhat difficult to prepare due to the larger thickness of the splats and the greater depth of the crater, showed that from the non-melted zones, no oxide phases or substrate melting were evident. However, for the locally melted zones, the features found were similar to the ones observed for the fully melted splats, which are described below.

Description of the Formation Process: The crater observed for the fully melted splat is present as well for the partially melted splats, suggesting that the formation process starts similarly as for the fully melted splats: the NiCr particle impacting the substrate in a partially melted state, with a solid core responsible for the deformation of the substrate (Fig. 5a). The non-melted fragments may then be from this non-melted core, which may have fragmented upon impact.

It is also very possible that some parts (melted or non-melted) rebound from the substrate. Indeed, for most of these partially melted splats, the NiCr phase barely fills the crater in the substrate, and the original sprayed particle must have been significantly larger than the crater created.

3.1.3 Effects of the Substrate Surface Heat Treatment. For both Al_P and Al_PT specimens, SEM images of 50-60 splats were recorded, and for each type of splat described above, the average value D_m of their diameter D and the relative population were evaluated. Evaluating the diameter was performed by taking the smallest and largest diameter value measured from the splat, which is not perfectly circular, and calculating the average value; features such as splashed fingers were ignored (see for example Fig. 1d). Results are summarized in Table 2. It should be noted that these values are broadly indicative as the number of splats studied is insufficient to calculate precise statistics of splat morphology. The impact craters with no NiCr present were not included in this analysis due to their relatively low frequency. Results for the boiled specimens were not included either, as the splats formed on those substrates are significantly different and will be discussed later.

Because of the relative imprecision of the values, it can be noted that the different types of splats have, on one hand, similar mean diameter that is the diameter of the crater, and, on the other hand, they are present on both specimens in approximately the same proportions.

Protective oxide layers naturally form on aluminum: an inner compact and amorphous oxide layer, covered with a

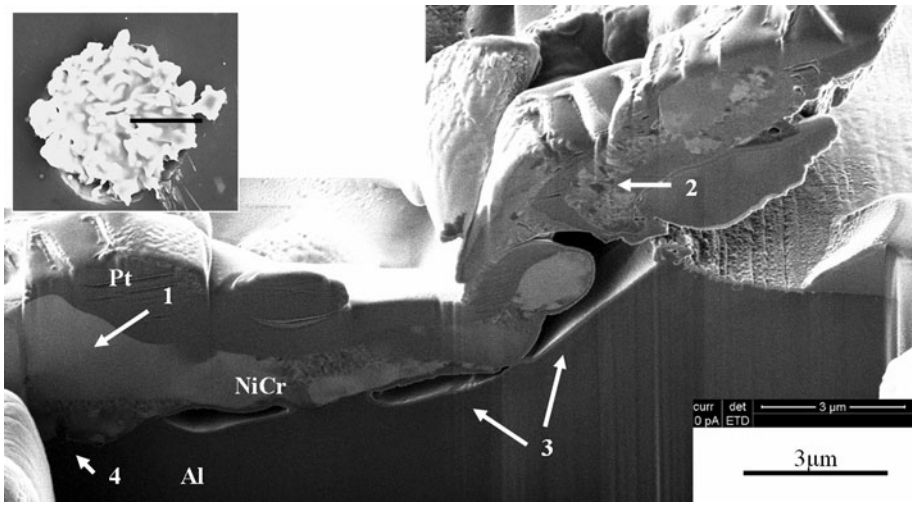

Fig. 6 FIB cross section of a partially melted splat (see inset image) on Al_PT

Table 2 Relative proportions and average diameters of the different types of splats found on the Al_P and Al_PT specimens

	Specimens	
	Al_P	**Al_PT**
Type of splat		
Unmelted/partially melted splat (Fig. 1b)	19% $D_m = [56.4 \pm 14.9]$ µm	17% $D_m = [54.4 \pm 10.9]$ µm
Fully melted splat, fragmented (Fig. 1c)	68% $D_m = [44.4 \pm 10.5]$ µm	64% $D_m = [42.7 \pm 12.3]$ µm
Fully melted splat, non fragmented (Fig. 1d/e)	13% $D_m = [48.5 \pm 21.3]$ µm	19% $D_m = [48.8 \pm 12.6]$ µm

more permeable layer of hydrated oxide (Ref 29, 30), reaching at room temperature a total thickness of 2-4 nm. The heat treatment applied (350 °C, 90 min in air) is expected to increase the oxide layer thickness up to about 7 nm, and may also cause dehydration of the outer oxide layer, possibly converting some of the hydroxide into oxide (Ref 31).

However, these changes in the surface chemistry of the substrate do not seem to have a significant influence on the splat shapes and, thus, the splat formation. This marks a substantial difference compared to plasma spraying, where similar heat treatments of the substrate before spraying were found to make the splats flatter and less fragmented, possibly by improving the wetting of the NiCr on the Al (Ref 14). This difference may be attributed to the difference in the temperatures and velocities with which the particle impacts on the substrate: In the plasma process, the particle velocity is lower and its temperature higher; thus the particle is fully melted upon impact, and the surface state may have a significant influence on the spreading of the melted NiCr. In the HVOF process, on the other hand, the higher velocity and lower temperature possibly means that, first, the substrate gets deformed, which may fragment or disrupt the oxide layers, and second, the pressure applied by the particle on the substrate upon splat formation is higher, as the way in which the melted NiCr wets the substrate surface is not influential.

3.2 Description of the Splats Found on the Boiled and Boiled and Thermally Treated Specimens

3.2.1 Description of the Splats Morphology and Microstructure. In previous studies of boiled Al specimens, it was shown that the boiling treatment produces a thick hydroxide layer (boehmite, AlOOH, about 300 nm in thickness) on the surface of the substrate (Ref 14, 15). Indeed, aluminum reacts with water in the following way: under 100 °C, bayerite α-$Al(OH)_3$ is expected to be formed; then above 100 °C, boehmite γ-AlOOH is the most likely hydroxide to be formed (Ref 32). Such a layer, present on both Al_B and Al_BT, is apparent as a dense homogenous dark layer on FIB cross sections, and was found to partially dehydrate upon heating, releasing water vapor. More details on these layers can be found in a study by the same authors (Ref 14).

Splats on both boiled and boiled and thermally treated specimens were overall similar in morphology, and examples are displayed in Fig. 7. In the crater shown in Fig. 7(a), a structure is seen, which is similar to the non-boiled specimens. However, some fragmented parts of melted NiCr can be found, arranged in a near-circular shape. The difference between the splats observed here, and those on the polished substrates, is the amount of NiCr that has adhered in the crater, ranging from a thin ring (Fig. 7a) to the crater being almost completely covered with NiCr (Fig. 7b, c).

Splats on Al_BT indicate that more NiCr adhered to the crater than for Al_B, and thicker splats, such as the one shown in Fig. 7(c), which were only found on Al_BT. No partially melted splats, as seen for Al_P and Al_PT, were found.

Figure 8 shows a FIB cross section of a typical splat. The crater here is about 5 μm deep (1), but compared to splats present on the non-boiled specimens, less NiCr has adhered to the substrate (2). Furthermore, the shape of the NiCr fragments and also the shape of their grains are quite irregular. Some lift-up of the Al substrate at the periphery of the crater can also be observed (3). The hydroxide layer produced by the boiling treatment, which exhibits a dark contrast on the FIB cross section can be observed here just outside the crater (4), and some thinner remnants of this layer can also be seen in the crater (5).

TEM examination of the splats, for example, the cross section presented in Fig. 9, confirms the presence of Al hydroxide: on one hand, EDS elemental maps (see Fig. 9b, d) confirm the presence of a layer rich in Al and O on top of the Al substrate; on the other hand, the electron diffraction pattern (see Fig. 9f) obtained from this layer presents rings that are consistent with boehmite γ-AlOOH (as described in a previous study (Ref 14). It should be noted that corundum Al_2O_3 presents a similar ring pattern to boehmite, and the two phases are not readily distinguished using electron diffraction. However, x-ray photoelectron spectroscopy (XPS) data suggested that the phase most likely to be present is γ-AlOOH (Ref 31). Furthermore, it can be noted that no NiCr is present on top of the Al hydroxide phase: the fragments of NiCr that have adhered to the substrate are directly in contact with the aluminum. In these regions, the contact between the splat and substrate is good, and the splat-substrate interface is irregular. The elemental EDS linescan performed across the interface in that area shows that, similarly to the Al_P and Al_PT substrates, Ni has diffused into the substrate to a depth of about 150 nm.

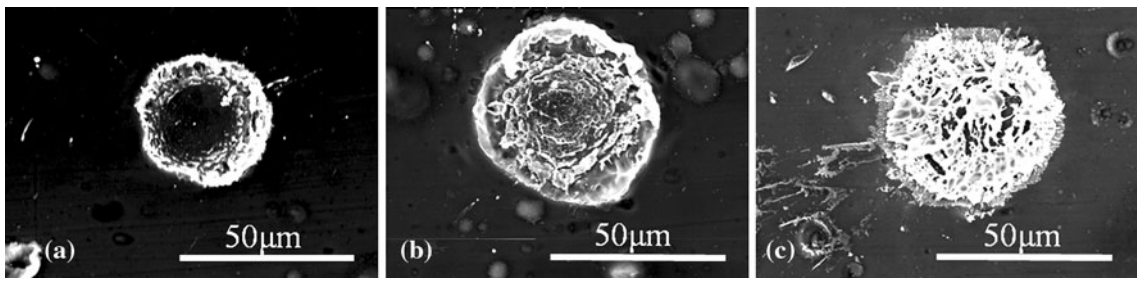

Fig. 7 SEM images of typical splats found on (a, b) Al_B and (a, b, c) Al_BT

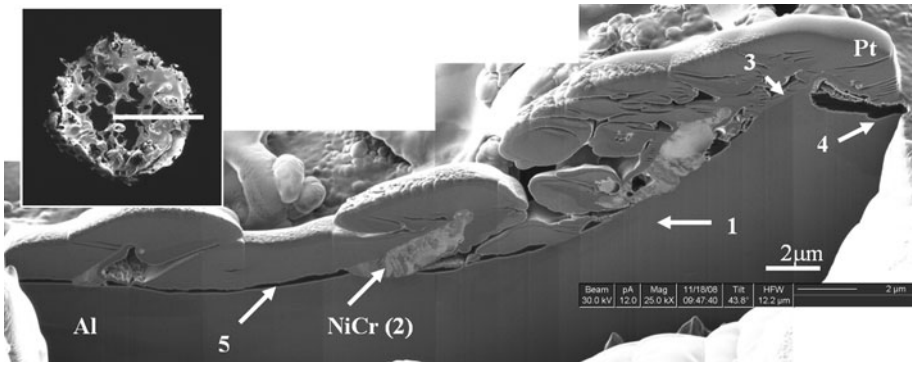

Fig. 8 FIB cross section of a fully melted splat (see inset image) on Al_BT

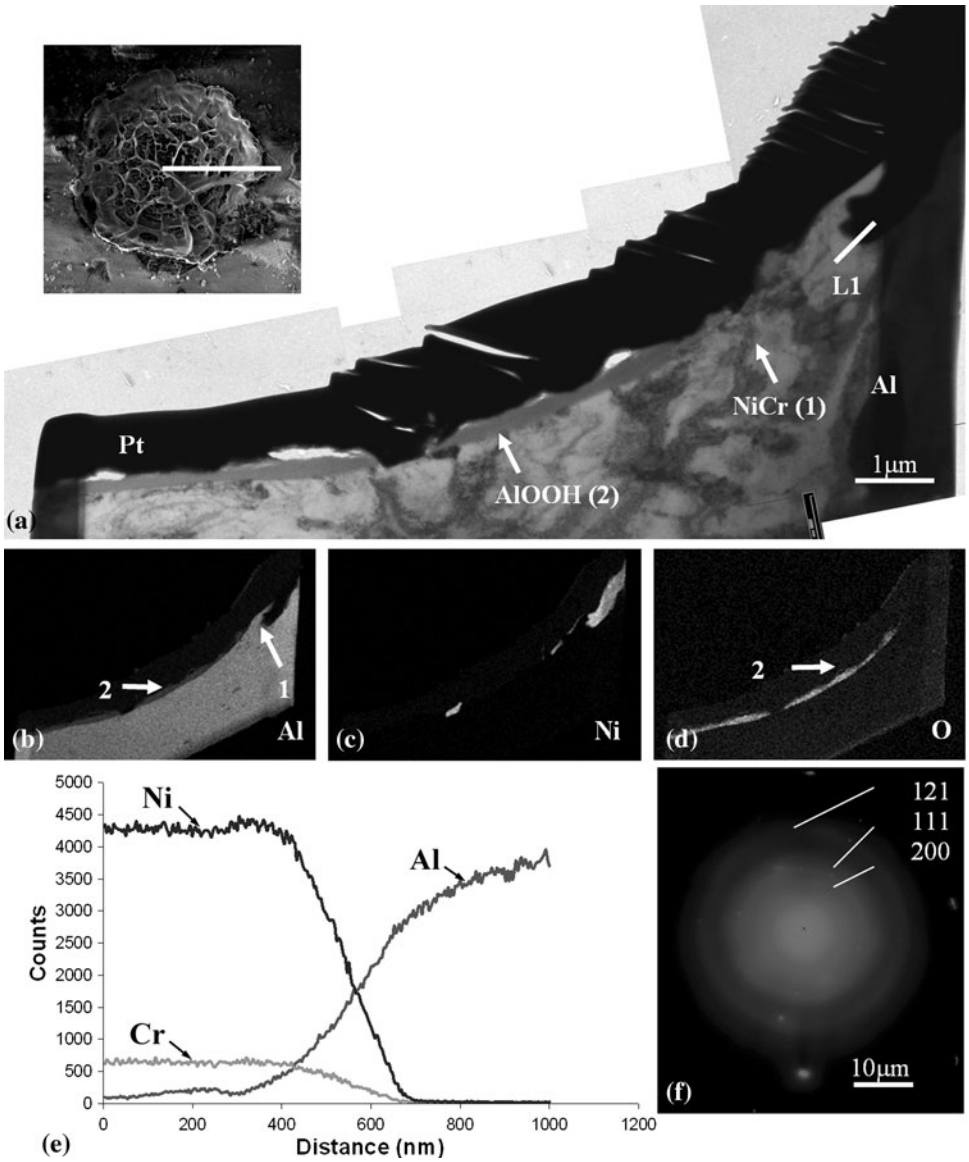

Fig. 9 TEM cross section of a typical splat (see inset image) found on Al_BT: (a) bright field image, EDS elemental maps for (b) Al, (c) Ni and (d) O, (e) elemental linescan made across the splat-substrate interface, (f) diffraction pattern of AlOOH

3.2.2 Splat Formation and Effects of the Boiling Treatment. It has been observed that on both boiled and boiled and thermally treated aluminum specimens, before spraying, a relatively thick (~300 nm) layer of hydroxide was present on the substrate surface. Such layer was also found to inhibit adhesion of splats in the case of plasma spraying, possibly due to the dehydration of the hydroxide layer from the heat from the spray process, causing the release of a significantly large amount of gas hinder the contact between NiCr and the Al substrate (Ref 14).

Here, FIB and TEM cross sections showed that the splat microstructure is similar to the one of the splats found on Al_P and Al_PT in several places, suggesting similarities in the splat formation process. The crater shows that the sprayed particle impacted in a partially melted state, and the solid core deformed the Al substrate, causing the crater formation observed. A limited amount of NiCr was also found to have adhered to the substrate. This was probably made possible by the partial destruction of the hydroxide layer by the NiCr particle impacting on the substrate with a high momentum. Indeed, such a layer was found to be much thinner and not uniform inside the craters. Moreover, no NiCr could be found where the hydroxide layer was present. It should be noted, however, that much less NiCr constitutes the splats on the boiled specimens compared with the non-boiled ones: even if it gets partially destroyed, the hydroxide layer does completely limit the adhesion of NiCr onto the substrate.

Where the hydroxide layer has been removed, similar to the case of the fully melted splats on Al_P and Al_PT, the high pressure build up from the impact of the high momentum particle along with the relatively high temperature of the melted NiCr allows very good contact between NiCr and Al and sometimes the localized melting of the substrate, which may then be jetted by the flowing movement of the splat, and mixed with the NiCr phase.

An important point of difference between boiled and non-boiled specimens is the absence of partially melted splats on the boiled specimens. However, it is expected that the breaking up of the solid core, which led on the polished substrates to the formation of partially melted splats, may also occur for the boiled substrates, and possibly with the same frequency. A possible explanation may be that the breaking up of the solid core upon impact means that the pressure applied by the particle on the substrate is not as high, thus the hydroxide layer remains and hinders splat adhesion. However, on Al_P and Al_PT it was seen that the crater for the partially melted splats was usually around the same dimension as the one for the fully melted splat: if deformation of the substrate occurs in the same way, this means that the pressure applied should be similar and disruption to the hydroxide layer should similarly occur. Another hypothesis may be that only the non-melted fragments did not adhere to the substrate and rebound like the solid core for the fully melted splats. This is in agreement with the observation that much less NiCr can be found in the splats on the boiled specimens compared to the non-boiled ones. Thus, insufficient melted NiCr is present to form the matrix in which the non-melted fragments may become embedded.

Finally, comparing splats between Al_B and Al_BT showed that on Al_BT the splats contained a higher volume fraction of NiCr (for example Fig. 7c). This may be explained by the heat treatment of Al_BT, which may have allowed a partial dehydration of the hydroxide layer, thus less gas would be released upon splat formation, and NiCr could have a better adhesion on the substrate, It is also possible that the heat treatment caused the hydroxide layer to be more brittle, leading to more damage upon impact by the sprayed particle.

In conclusion, while the thermal treatment at 350 °C was observed to have a limited effect on splat formation, the boiling treatment had a strong influence on the adhesion of the splats.

3.3 Comparison Between HVOF and Plasma Sprayed Splats

When comparing the results obtained in this study with the plasma spraying of NiCr particles onto similar substrates, which were studied previously by the same authors (Ref 14), it can be noted that the splats formed are significantly different in morphology. On one hand, in the case of plasma spraying, there were no signs of substrate deformation or melting, with usually quite a poor contact between splat and substrate. However, some authors have found that substrate melting could occur, when plasma spraying Ni and Cr onto Al substrates, for instance, Kitahara and Hasui (Ref 18), or when plasma spraying NiCr on stainless steel (Ref 27). On the other hand, there was no sign for plasma-sprayed splats that most of the sprayed particle would rebound for the substrate, as seen for HVOF. Nevertheless, upon subsequent spraying passes, it is expected that rebound of the NiCr particle would cease, as NiCr coatings are often sprayed onto Al by HVOF (Ref 1).

Concerning the effects of surface chemistry, in the case of plasma spraying, heat treating the Al substrate slightly increased the wetting of NiCr, giving splats a more circular and flatter morphology, and boiling completely prevented any splat to adhere on the substrate (Ref 14). For the HVOF process, it can be noted that the effects of the pre-treatments, and, thus, the changes in the surface chemistry they create, are weaker. A possible explanation is that due to the lower temperature and higher velocity of the sprayed particles, and the partially melted state in which they impact on the substrate, the influence of elements such as wetting and gas desorption is hindered by the fact that the particle impacts the substrate with a high momentum, thereby applying a high pressure to it. Moreover, from the deformation of the substrate, the layers formed by the pre-treatments tend to be altered, thus NiCr may interact more directly with the Al substrate, without the presence of oxides or hydroxides. Research is currently being performed on splats sprayed in different conditions to bring further insight into these hypotheses.

4. Conclusion

In summary, NiCr was HVOF sprayed onto Al substrates having undergone various pre-treatments (boiling and heating) which modified their surface chemistry. The following observations were made:

- For all specimens, the NiCr particles impacted the substrate in a partially molten state. The solid core deformed the substrate, creating a crater in which only a small portion of NiCr particle adhered to the substrate. Where effective contact between molten NiCr and Al was achieved, substrate melting often occurred: the molten aluminum may then be jetted within the splat and/or lifted up at the periphery of the crater, and at the splat substrate interface, the mixing of both phases may lead to particular very finely grained microstructure made of a mixture of Ni and Al grains. Cr_2O_3 was found to form as a thin layer on the outer surface of the splats, and in some pores at the splat-substrate interface, NiO or $NiCr_2O_4$ may form, as well. Some splats were also found to be made of a mixture of non-melted fragments in a melted matrix of NiCr, but they were absent from the boiled specimens.
- The thermal treatment is expected to increase the thickness of the Al_2O_3 layer present on top of the substrate, and was found to increase the amount of molten NiCr that adheres to the substrate.
- The boiling treatment created a thick and dense boehmite layer on top of the Al substrate, which significantly limited the amount of NiCr adhering on the substrate.

Consequently, using electron microscopy to study the splat microstructure at a nano-scale level allowed a new insight on the mechanisms of splat formation, while it was shown that substrate surface conditions can be a significantly important parameter regarding the influence on splat formation and thus the performances of the fully deposited coating.

References

1. R.F. Bunshah, *Handbook of Hard Coatings. Deposition Technologies, Properties and Applications*, Noyes Publications, Norwich, NY, 2001
2. M. Dorfman, Thermal Spray Basics, *Adv. Mater. Process.*, 2002, July, p 47-50
3. W.J. Trompetter, M. Hyland, D. McGrouther, P. Munroe, and A. Markwitz, Effect of Substrate Hardness on Splat Morphology in High-Velocity Thermal Spray Coatings, *J. Therm. Spray Technol.*, 2006, **15**(4), p 663-669
4. P. Bansal, P.H. Shipway, and S.B. Leen, Effect of Particle Impact on Residual Stress Development in HVOF Sprayed Coatings, *J. Therm. Spray Technol.*, 2006, **15**(4), p 570-575
5. C.J. Kong, P.D. Brown, S.J. Harris, and D.G. McCartney, The Microsctructure of a Thermally Sprayed and Heat Treated Al-20wt.%Sn-3wt.%Si Alloy, *Mater. Sci. Eng. A*, 2005, **403**, p 205-214
6. T. Marrocco, L.C. Driver, S.J. Harris, and D.G. McCartney, Microstructure and Properties of Thermally Sprayed Al-Sn-Based Alloys for Plain Bearing Applications, *J. Therm. Spray Technol.*, 2006, **15**(4), p 634-639
7. P. Fauchais, M. Fukumoto, A. Vardelle, and M. Vardelle, Knowledge Concerning Splat Formation: An Invited Review, *J. Therm. Spray Technol.*, 2004, **13**(3), p 337-360
8. S.V. Klinkov, V.F. Kosarev, and M. Rein, Cold Spray Deposition: Significance of Particle Impact Phenomena, *Aerosp. Sci. Technol.*, 2005, **9**, p 582-591
9. R.C. Dykhuizen, M.F. Smith, D.L. Gilmore, R.A. Neiser, X. Jiang, and S. Sampath, Impact of High Velocity Cold Spray Particles, *J. Therm. Spray Technol.*, 1999, **8**(4), p 559-564
10. L. Ajdelsztajn, A. Zúñiga, B. Jodoin, and E.J. Lavernia, Cold Gas Spraying of a High Temperature Al Alloy, *Surf. Coat. Technol.*, 2006, **201**, p 2109-2116
11. J.M. Guilemany, J. Nutting, J.R. Miguel, and Z. Dong, Microstructure Characterization of WC-Ni Coatings Obtained by HVOF Thermal Spraying, *Scr. Metall. Mater.*, 1995, **33**(1), p 55-61
12. V.V. Sobolev and J.M. Guilemany, Effect of Oxidation on Droplet Flattening and Splat-Substrate Interaction in Thermal Spraying, *J. Therm. Spray Technol.*, 1999, **8**(4), p 523-530
13. J. Cedelle, M. Vardelle, and P. Fauchais, Influence of Stainless Steel Substrate Preheating on Surface Topography and on Millimeter- and Micrometer-Sized Splat Formation, *Surf. Coat. Technol.*, 2006, **201**, p 1373-1382
14. S. Brossard, A.T.T. Tran, P.R. Munroe, and M.M. Hyland, Study of the Splat Formation for Plasma Sprayed NiCr on an Al5052 Substrate as a Function of Substrate Condition, Submitted to *Surf. Coat. Technol.*, 2009. doi:10.1016/j.surfcoat.2010.02.013
15. A.T.T. Tran and M.M. Hyland, The Role of Substrate Surface Chemistry on Splat Formation During Plasma Spray Deposition by Experiments and Simulations, *J. Therm. Spray Technol.*, 2010, **19**(1-2), p 11-23
16. P.R. Munroe, The Application of Focused Ion Beam Microscopy in the Material Sciences, *Mater. Charact.*, 2009, **60**, p 2-13
17. T.B. Massalski, H. Okamoto, P.R. Subramanian, and L. Kacprzak, *Binary Alloy Phase Diagrams*, 2nd ed., ASM International, Materials Park, OH, 1990
18. S. Kitahara and A. Hasui, A Study of the Bonding Mechanism of Sprayed Coatings, *J. Vac. Sci. Technol.*, 1974, **11**(4), p 747-753
19. B. Wielage, A. Wank, H. Pokhmurska, T. Grund, C. Rupprecht, G. Reisel, and E. Friesen, Development and Trends in HVOF Spraying Technology, *Surf. Coat. Technol.*, 2006, **201**, p 2032-2037
20. R.S. Lima and B.R. Marple, Optimized HVOF Titania Coatings, *J. Therm. Spray Technol.*, 2003, **12**(3), p 360-369
21. D. Zhang, S.J. Harris, and D.G. McCartney, Microstructure Formation and Corrosion Behaviour in HVOF-Sprayed Inconel 625 Coatings, *Mater. Sci. Eng. A*, 2003, **344**, p 45-56
22. N.Z. Mehdizadeh, M. Lamontagne, C. Moreau, S. Chandra, and J. Mostaghimi, Photographing Impact of Molten Molybdenum Particles in a Plasma Spray, *J. Therm. Spray Technol.*, 2005, **14**(3), p 354-361
23. K. Shinoda, H. Murakami, S. Kuroda, S. Oki, K. Takehara, and T.G. Etoh, High-Speed Thermal Imaging of Yttria-Stabilized Zirconia Droplet Impinging on Substrate in Plasma Spraying, *Appl. Phys. Lett.*, 2007, **90**, p 194103-1-194103-3
24. X.Y. Jiang, Y. Wan, H. Herman, and S. Sampath, Role of Condensate and Adsorbates on Substrate Surface on Fragmentation of Impinging Molten Droplets During Thermal Spray, *Thin Solid Films*, 2001, **385**, p 132-141
25. W.J. Trompetter, M. Hyland, P. Munroe, and A. Markwitz, Evidence of Mechanical Interlocking of NiCr Particles Thermally Sprayed onto Al Substrates, *J. Therm. Spray Technol.*, 2005, **14**(4), p 524-529
26. S. Brossard, P.R. Munroe, A.T.T. Tran, and M.M. Hyland, Study of the Effects of Surface Chemistry on Splat Formation for Plasma Sprayed NiCr onto Stainless Steel Substrates, *Surf. Coat. Technol.*, 2009, **204**(9-10), p 1599-1607
27. S. Brossard, P.R. Munroe, A.T.T. Tran, and M.M. Hyland, Study of the Microstructure of NiCr Splats Plasma Sprayed on Stainless Steel by TEM, *Surf. Coat. Technol.*, 2009, **204**(9-10), p 1608-1615
28. S. Brossard, A.T.T. Tran, P.R. Munroe, and M.M. Hyland, Study of the Splat-Substrate Interface for a NiCr Coating Plasma Sprayed onto Polished Aluminum and Stainless Steel Substrates, *J. Therm. Spray Technol.*, 2010, **19**(1), p 24-30

29. J.R. Davis, *Aluminum and Aluminum Alloys*, ASM International, Materials Park, OH, 1993
30. M.S. Hunter and P. Fowle, Natural and Thermally Formed Oxide Films on Aluminum, *J. Electrochem. Soc.*, 1956, **103**(9), p 482-485
31. A.T.T. Tran, M.M. Hyland, T. Qiu, B. Withy, and B.J. James, Effect of Surface Chemistry on Splat Formation During Plasma Spraying, *J. Therm. Spray Technol.*, 2008, **17**(5-6), p 637-645
32. R.S. Alwitt, Aluminium-Water System, *Oxid. Oxid. Films*, 1976, **4**, p 169-254